Effects of Pressure Gradients on Energy Dissipation Coefficient

Soheil Soleimani[1,*], E. Ghasemi[1] and M.A. Almas[1,2]

[1]*Department of Mechanical and Materials Engineering, Florida International University, Miami, FL 33199, USA*

[2]*Department of Marine engineering, King Abdulaziz University, 21589, Saudi Arabia*

Abstract: In this study energy dissipation coefficient and entropy generation process in characteristic wall shear flows have been investigated. Effect of pressure gradients on energy dissipation coefficient for flows undergoing "bypass" transition from laminar to turbulent state has been studied. Reynolds-Averaged Navier-Stokes (RANS) models and Direct Numerical Simulations (DNS) are implemented to study the energy dissipation coefficient and local entropy generation in pre-transitional and transitional regions. Three of these RANS models are transitional models such as, traditional SST $k-\omega$ (2eq), SST $k-\omega$ (4eq) and $k-kl-\omega$ and the results are compared with DNS. Four simulations have been performed for (1) zero, (2) favorable, (3) adverse and (4) strong-adverse pressure gradient cases. The numerical results show that the pressure gradient has a significant effect on energy dissipation coefficient and entropy generation.

Keywords: Energy dissipation coefficient, entropy generation, pressure gradients, transitional boundary layer, bypass transition, rans Models.

1. INTRODUCTION

Fundamental understanding of local (pointwise) distributions of entropy generation rates and energy dissipation coefficient in characteristic wall shear flows are significant to potentially increasing energy efficiency and sustainability and thereby reducing fuel consumption [1]. For entropy generated by fluid friction, the rates are predictable for developed turbulent flows and pure laminar flows as reported by McEligot *et al.* [2-4]. The main difficulty lies in prediction of flows undergoing a so-called "bypass" transition [5-7] from a laminar to a turbulent state induced by strong freestream turbulence and streamwise pressure gradients. Most of the work to date have been on investigating the flow field using direct numerical simulation and very few studied have been done on investigating the entropy generation and energy dissipation coefficient in such flow fields; fewer studies considered turbulence models like RANS [5-7] to examine the capability and versatility of such industrial turbulence models since the applications of DNS are confined to the flow field with low Reynolds number. Almost all of these works have not considered the effect of pressure gradients which have an important influence on such type of flows. Thus a study on entropy generation and energy dissipation coefficient employing different turbulence models were deemed of interest. E. Ghasemi *et al*. [5] studied the entropy generation in a transitional boundary layer region under the influence of freestream turbulence numerically for zero pressure gradient case. As their results [5] show, all the RANS models which they studied predicted transition onset prematurely and, consequently, over predict the integral entropy generation rate and the skin friction coefficient in the transition region; and also their results show that among the RANS models, SST $k-\omega$ (4eq) model and $k-kl-\omega$ provide the better results and SST $k-\omega$ (4eq) model predicts the transition onset closer to DNS. E. Ghasemi *et al*. [5] results clearly show that how entropy generation evolves in the transition from laminar to turbulent and the rate of entropy generation in transition region is much greater than that value in the other regions (laminar and turbulent). E. Ghasemi *et al*. [5] investigated an approximate equation for pointwise entropy generation and energy dissipation coefficient; their results provide a very good estimate of evaluating the rate of entropy and energy dissipation coefficient which significantly reduces the computational cost for numerical methods to calculate the fluctuation velocities in the region very close to wall. In continuation of their work E. Ghasemi *et al*. [6,7] studied the effects of adverse and favorable pressure gradients on entropy generation. Their results show that transition is early and abrupt for the strong adverse pressure gradient but occurs further downstream and is longer with the increasingly favorable flows, and that entropy generation rate at the wall increases as pressure gradient grows.

The objectives of the present research is to perform a study on effects of pressure gradients on energy dissipation coefficient and entropy generation in a

*Address correspondence to this author at the Department of Mechanical and Materials Engineering, Florida International University, Miami, FL 33199, USA; Tel: +1(786)202-3565; Fax: (305)348-1932; E-mail: ssole016@fiu.edu

E-ISSN: 2409-5826/14

transitional boundary layer region over a flat plate under the influence of free stream turbulence.. Study of pressure gradient effects on entropy generation and energy dissipation coefficient have been performed for different cases of favorable, zero, adverse and strong-adverse pressure gradients. Numerical results of the turbulence RANS models have been compared to the DNS data to examine the accuracy of these models in modeling such flow fields which have a variety of industrial and engineering applications.

2. ENERGY DISSIPATION COEFFICIENT (C_d)

The entropy generation rate per unit area S'' is a key quantity for minimizing thermodynamic losses for overall design. In wall coordinates, it can be written as [5-7],

$$\left(S''\right)^+ = \frac{TS''}{\rho u_\tau^{\,3}} = \int_0^{y^+} \left(S'''\left\{y^+\right\}\right)^+ dy^+ \tag{1}$$

If the pointwise mean turbulence kinetic energy equation is integrated from the wall to the free stream - subject to the presence of free stream turbulence at the edge of the boundary layer – and the direct dissipation is added, the following can be derived as [8,9],

$$\begin{aligned}\left(S''\left\{\delta\right\}\right)^+ \approx{}& \int_0^\delta \left(\partial U^+/\partial y^+\right)^2 dy^+ - \int_0^\delta \left(\overline{uv}\right)^+ \left(\partial U^+/\partial y^+\right) \\ & dy^+ - \int_0^\delta \left[\overline{\left(u^2\right)^+} - \overline{\left(v^2\right)^+}\right]\left(\partial U^+/\partial x^+\right) dy^+ - \left(d/dx^+\right) \\ & \int_0^\delta U^+ \left(1/2\right)\left(\overline{q^2}\right)^+ dy^+ - \left(1/2\right)\overline{v_\delta^+ \left[\left(u_\delta^{\,2}\right)^+ + \left(v_\delta^{\,2}\right)^+ + \left(w_\delta^{\,2}\right)^+\right]} - \overline{v_\delta^+ p_\delta^+}\end{aligned} \tag{2}$$

In terms of freestream velocity, U_∞, the entropy generation rate per unit area $\left(S''\right)^+$ may be written as an energy dissipation coefficient [8,9]

$$C_d = \frac{TS''}{\rho U_\infty^{\,3}} = \left(S''\left\{\delta\right\}\right)^+ \left(C_f/2\right)^{3/2} \tag{3}$$

3. NUMERICAL SIMULATIONS AND BOUNDARY CONDITIONS

The results of direct numerical simulation by Nolan and Zaki [10] are employed as benchmarks to assess the possible use of popular turbulence and transition models to predict entropy generation in bypass transition. The flow domain and boundary conditions are the same as those in E. Ghasemi *et al*. [5-7]. The grid spacing is uniform in the streamwise and clustered inside the boundary layer in the wall-normal direction. ASYSY-FLUENT is used for applying RANS and transitional models. The Finite-Volume (FV) approach using the SIMPLE algorithm is used with second-order upwind differencing for the convective terms and the central differencing for diffusion terms.

4. RESULTS AND DISCUSSIONS

4.1. Zero Pressure Gradient

Figure **1** demonstrates the DNS prediction of the different terms contributing to the energy dissipation rate in Eq. (2). At the beginning of the computational domain, at $Re_{\delta 0} =$ 800 where the velocity profile is laminar with very small fluctuations, the Blasius and DNS solutions nearly agree since the turbulent portion is still essentially zero.

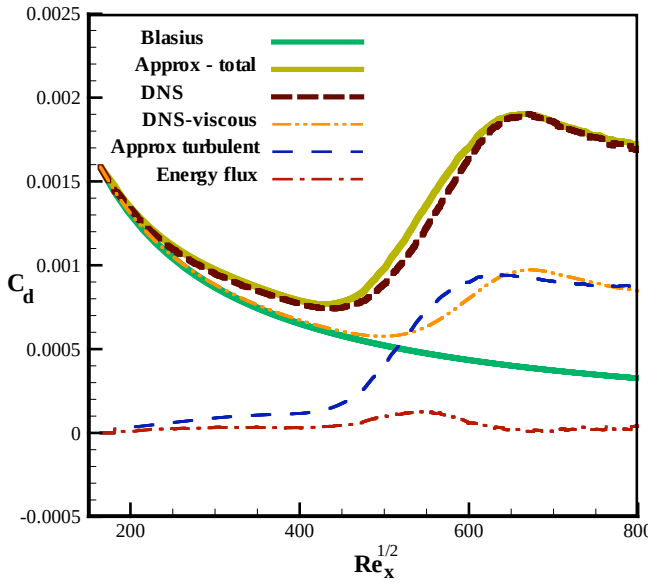

Figure 1: DNS results for dissipation coefficient C_d and related contributions.

As the flow develops the mean velocity profile deviates from the Blasius solution due to variation of the viscous term contribution. The quasi-turbulent contribution to C_d is enhanced in the pre-transitional region as the freestream turbulence initiates streaks growing inside the boundary layer. As seen from the Figure the contribution of the turbulent fluctuation is slightly greater than the viscous one in part of the transition region. There is a difference between 'approx-total DNS' and the exact DNS within the transition region that shows the contribution of the energy flux term in the energy dissipation equation. This energy flux term is first noticeable in the pre-transitional laminar boundary layer. It then grows to about ten per cent of C_d. As the developed turbulent boundary layer is approached it decreases and becomes negligible. This behavior is consistent with the observations of Walsh *et al*. [11]; their higher

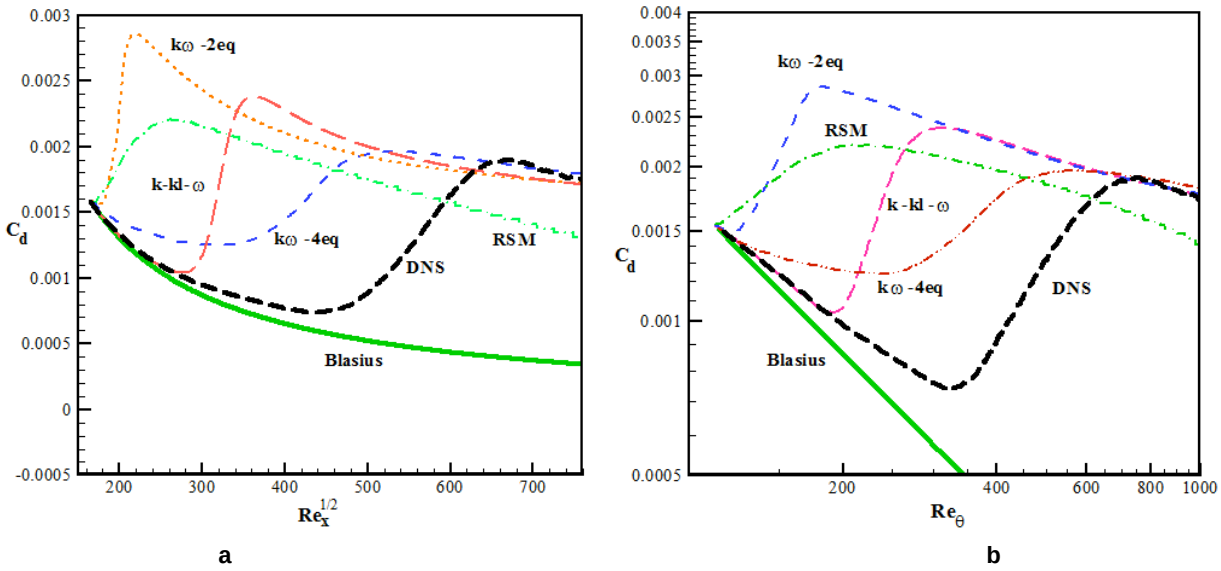

a **b**

Figure 2: Comparison of dissipation coefficients C_d calculated by RANS models with total C_d by DNS.

freestream turbulence (Tu_{in} = 4.7 %) apparently led to a somewhat larger contribution from this energy flux term. The present RANS predictions of C_d are compared to the DNS results and Blasius predictions in Figure **2** in two formats for the reader's convenience.

As with C_f, predictions for the two turbulence models diverged from the pure laminar case almost immediately. The two transition models diverged more gradually, consistent with their later apparent transition onset, but still much sooner than the DNS. Consequently, all these RANS models overpredict the entropy generation rate in the transition region. For Re_θ greater than about 700, all except the RSM agree with the DNS results for the developed turbulent boundary layer [5-7, 12].

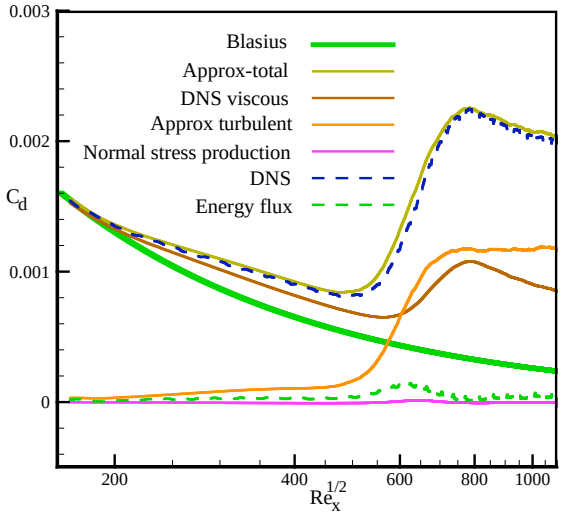

Figure 3: DNS results for dissipation coefficient C_d and related contributions.

The results of the present study can be extended by using LES modeling of turbulence flow [13-15], analytical modeling of boundary layer flow [16-23] or free convection heat transfer [24-29] using various numerical methods [30-33].

5. RESULTS FOR THE EFFECTS OF PRESSURE GRADIENTS

5.1. Favorable Pressure Gradient

Figure **3** demonstrates the DNS prediction of the different terms contributing to the energy dissipation rate in Eq. (2) for the FPG case. At the beginning of the computational domain, at Re_{δ_0} = 800 where the velocity profile is laminar with very small fluctuations, the Blasius and DNS solutions nearly agree since the turbulent portion is still essentially zero. As the flow develops the mean velocity profile deviates from the Blasius solution due to variation of the viscous term contribution. The quasi-turbulent contribution to C_d is enhanced in the pre-transitional region as the freestream turbulence initiates streaks growing inside the boundary layer. As seen from the Figure the contribution of the turbulent fluctuation is slightly greater than the viscous one in part of the transition region. As can be seen from the Figure, the values of different terms are slightly greater that those values for the ZPG case which is due to the effects of favorable pressure gradient or decreasing the pressure gradient effects. There is a difference between 'approx-total DNS' and the exact DNS within the transition region that shows the contribution of the energy flux term in the energy dissipation equation. This energy flux term

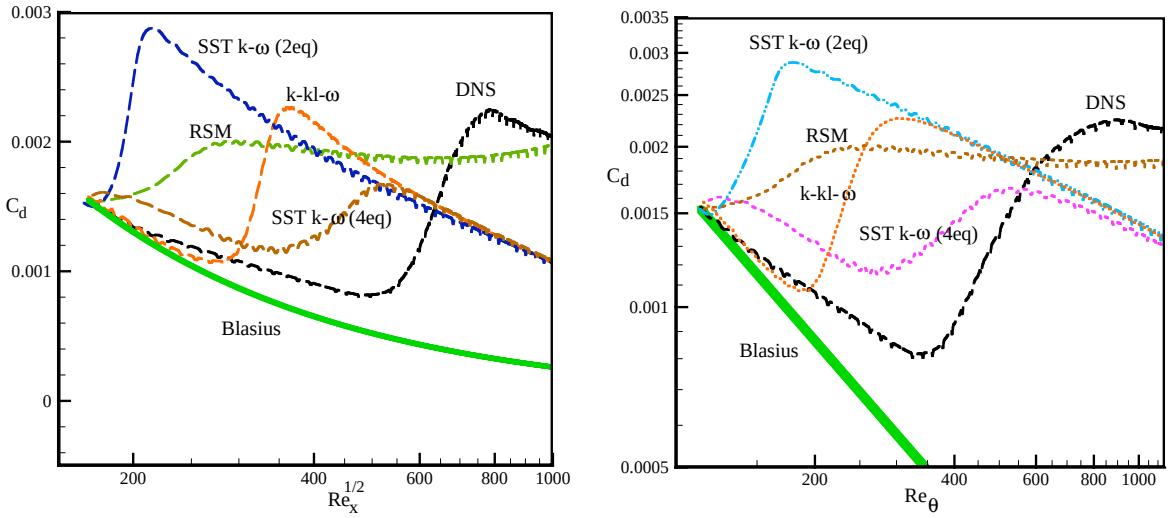

Figure 4: Comparison of dissipation coefficients C_d calculated by RANS models with total C_d by DNS.

is first noticeable in the pre-transitional laminar boundary layer. It then grows to about 10% of C_d. As the developed turbulent boundary layer is approached it decreases and becomes negligible. The present RANS predictions of C_d are compared to the DNS results and Blasius predictions in Figure **4** for the FPG case. As with C_f, predictions for the two turbulence models diverged from the pure laminar case almost immediately. The two transition models diverged more gradually, consistent with their delayed transition onset, but still much earlier than the DNS. Again compared to the ZPG case the DNS values of the FPG case are higher than the values for the ZPG case. Consequently, all these RANS models overpredict the entropy generation rate in the transition region. For Re_θ greater than about 800, none of them except the RSM agree with the DNS results for the developed turbulent boundary layer.

5.2. Adverse Pressure Gradient and Strong Adverse Pressure Gradient

Figure **5** demonstrates the DNS prediction of the different terms contributing to the energy dissipation rate for the APG cases. At the beginning of the computational domain, at Re_{δ_0} = 800 where the velocity profile is laminar from a ZPG (Blasius) with very small fluctuations, the Blasius and DNS solutions nearly agree since the turbulent portion is still essentially zero. As the flow develops the mean velocity profile deviates from the Blasius solution due to

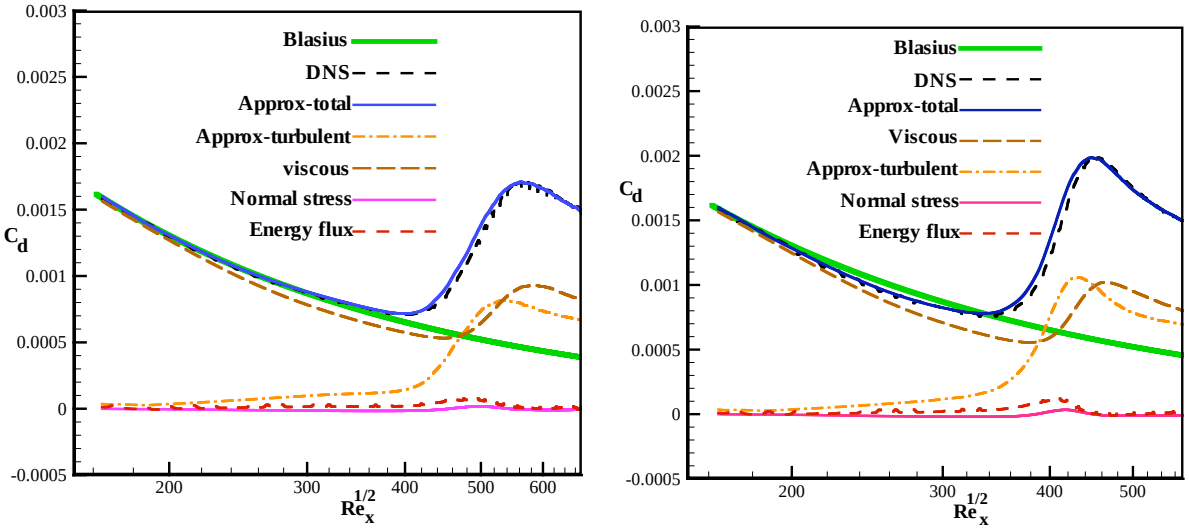

Figure 5: DNS results for dissipation coefficient C_d and related contributions, Top: APG , Bottom: APG_{strong} .

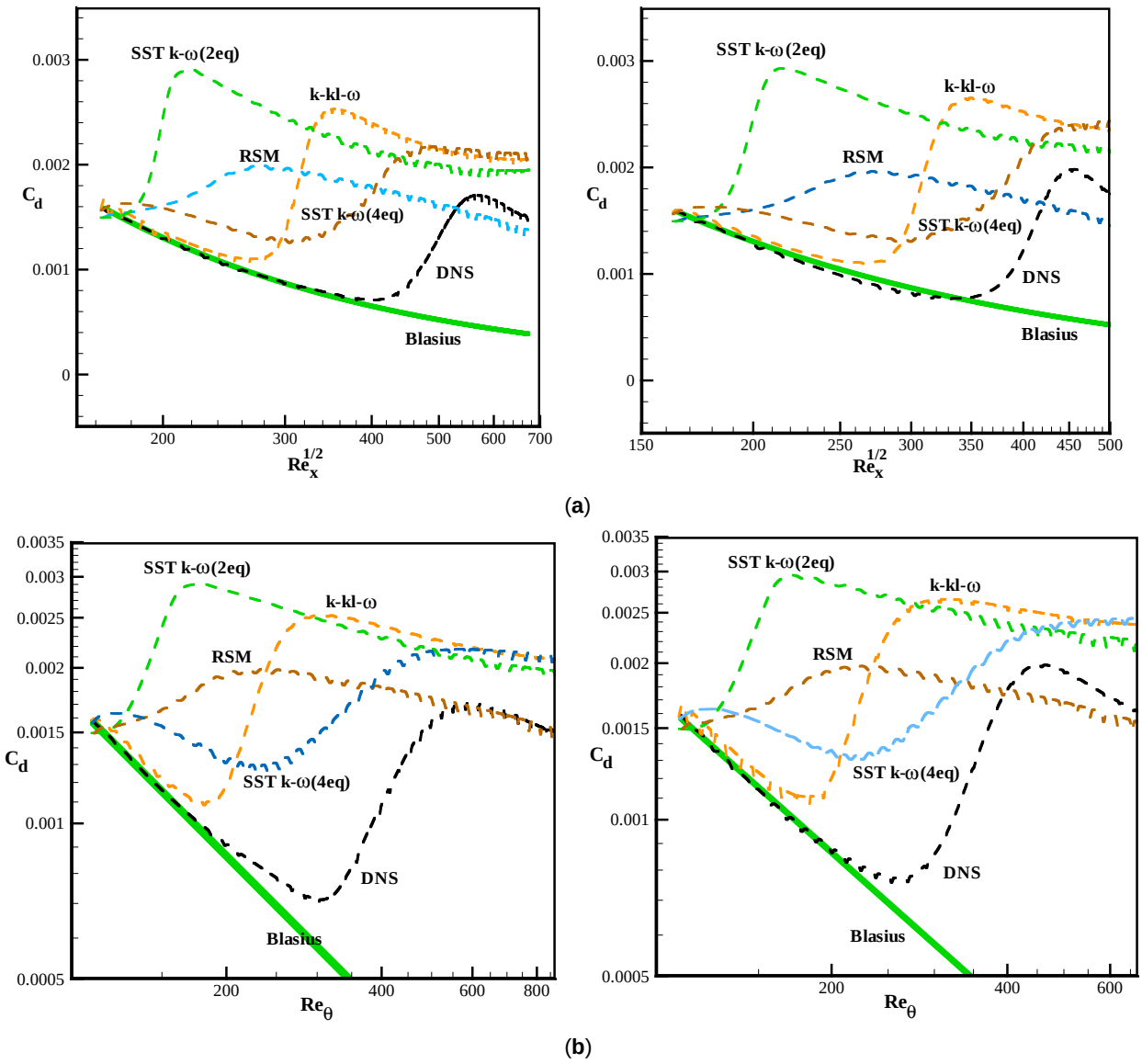

Figure 6: a: Comparison of dissipation coefficients C_d calculated by RANS models with total C_d by DNS. Top: APG, Bottom: APG_{strong} . **b:** Comparison of dissipation coefficients C_d calculated by RANS models with total C_d by DNS. Top: APG , Bottom: APG_{strong} .

variation of the viscous term contribution and pressure gradient. The quasi-turbulent contribution to C_d is enhanced in the pre-transitional region as the freestream turbulence initiates streaks growing inside the boundary layer. As can be seen from the Figure, the values of different terms are slightly lower than those values for the other cases which are due to the effects of adverse pressure gradients or increasing the pressure gradient effects. The present RANS predictions of C_d are compared to the DNS results and Blasius predictions in Figure **6** for the APG cases. As with C_f , predictions for the two turbulence models diverged from the Blasius case almost immediately. The two transition models diverged more gradually, consistent with their delayed transition onset, but still much sooner than the DNS. Compared to the ZPG and FPG cases, the DNS values of the APG case is smaller than that value for the ZPG case, but for APG_{strong} it is almost the same as ZPG case.

6. CONCLUSIONS

Here, five RANS models ($k-\varepsilon$ enhanced wall, SST $k-\omega$ (2eq), SST $k-\omega$ (4eq), $k-kl-\omega$ and RSM) have been implemented to study the energy dissipation coefficient and entropy generation in a transitional boundary layer region for flow over a flat plate, under the influence of free stream turbulence.

Study of pressure gradient effects on energy dissipation coefficient and entropy generation have been investigated for different cases of favorable, zero, adverse, and strong-adverse pressure gradients (FPG, ZPG, APG and strong APG). Numerical results of the turbulence RANS model based simulation have been compared to DNS data to examine the accuracy of these models in modeling such flow fields. All the RANS models over predict the energy dissipation coefficient and the integral entropy generation rate in the transition region.

ACKNOWLEDGEMENTS

The third author would like to thank both the Saudi Arabian Cultural Mission in Washington D.C. and King Abdulaziz University in Jeddah, KSA for their support.

REFERENCES

[1] Rose MG. What should we measure? An aero-engine turbine aero-dynamic perspective. XIV Bi-annual Symp. Meas. Techniques in Transonic and Supersonic Flow in Cascades and Turbomachines, Limerick, September, 1998.

[2] McEligot DM, Walsh EJ, Laurien E, Spalart PR, Entropy generation in the viscous parts of a turbulent boundary layer. J Fluids Eng. 2008; 130: 061205-1 to -12.

[3] McEligot DM, Nolan KP, Walsh EJ, Laurien E. Effect of pressure gradients on entropy generation in the viscous layers of turbulent wall flows. Int J Heat Mass Transfer 2008; 51: 1104-1114. http://dx.doi.org/10.1016/j.ijheatmasstransfer.2007.05.008

[4] McEligot DM, Brodkey RS, Eckelmann H. Laterally converging duct flows: Part 4. Temporal behavior in the viscous layer. J. Fluid Mech 2009; 634: 433-461. http://dx.doi.org/10.1017/S0022112009006727

[5] Ghasemi E, McEligot DM, Nolan KP, Crepeau J, Tokuhiro A, Budwig RS, Entropy generation in a transitional boundary layer region under the influence of freestream turbulence using transitional RANS models and DNS. International Communications in Heat and Mass Transfer 2013; 41: 10-16. http://dx.doi.org/10.1016/j.icheatmasstransfer.2012.11.005

[6] Ghasemi E, McEligot DM, Nolan KP, Crepeau J, Siahpush A, Budwig RS, Tokuhiro A. Effects of adverse and favorable pressure gradients on entropy generation in a transitional boundary layer region under the influence of freestream turbulence. International Journal of Heat and Mass Transfer 2014; 77: 475-488. http://dx.doi.org/10.1016/j.ijheatmasstransfer.2014.05.028

[7] Ghasemisahebi E. Entropy generation in transitional boundary layers. LAP LAMBERT Academic Publishing 2013.

[8] Rotta JC. Turbulent boundary layers in incompressible flow. Prog. Aero. Sci 2. Oxford: Pergamon Press 1962.

[9] Schlichting H. Boundary layer theory, 6th ed. New York McGraw-Hill 1968.

[10] Nolan KP, Zaki TA. Conditional Sampling of Transitional Boundary Layers in Pressure Gradients. J Fluid Mech 2013; 728: 306-339. http://dx.doi.org/10.1017/jfm.2013.287

[11] Walsh EJ, McEligot DM, Brandt L, Schlatter P. Entropy generation in boundary layers transitioning under the influence of freestream turbulence. J Fluids Eng 2011; 133: 061203-1-10 -10.

[12] Nolan K, Walsh EJ, McEligot DM, Volino RJ. Predicting entropy generation rates in transitional boundary layers based on intermittency. J. Turbomachinery 2007; 129(3): 512-517. http://dx.doi.org/10.1115/1.2720488

[13] Taeibi-Rahni M, Ramezanizadeh M, Ganji DD, Darvan A, Ghasemi E, Soleimani S, Bararni H. Large-eddy simulations of three dimensional turbulent jet in a cross flow using a dynamic subgrid-scale eddy viscosity model with a global model coefficient. World Appl Sci J 2010; 9: 1191-1200.

[14] Taeibi-Rahni M, Ramezanizadeh M, Ganji DD, Darvan A, Ghasemi E, Soleimani S, Bararni H, Large-eddy simulations of three dimensional turbulent jet in a cross flow using a dynamic subgrid-scale eddy viscosity model with a global model coefficient. World Appl Sci J 2010; 9: 1191-1200.

[15] Taeibi-Rahni M, Ramezanizadeh M, Ganji DD, Darvan A, Ghasemi E, Soleimani S, Bararni H. Comparative study of large eddy simulation of film cooling using a dynamic global-coefficient subgrid scale eddy-viscosity model with RANS and Smagorinsky Modeling. Int. Commun. Heat. Mass. Trans 2011; 38: 659-667. http://dx.doi.org/10.1016/j.icheatmasstransfer.2011.02.002

[16] Ghasemi E, Bayat M, Bayat M. Visco-Elastic MHD flow of Walters liquid b fluid and heat transfer over a non-isothermal stretching sheet. International Journal of Physical Sciences 2011; 6(21): 5022-5039.

[17] Ghasemi E, Soleimani S, Bararnia H, Domairry G. Influence of Uniform Suction/Injection on Heat Transfer of MHD Hiemenz Flow in Porous Media. ASCE Journal of Engineering Mechanics 2012; 138(1): 82-88. http://dx.doi.org/10.1061/(ASCE)EM.1943-7889.0000301

[18] Bararnia H, Ghasemi E, Soleimani S, Baraei A, Ganji DD. HPM-Padé method on natural convection of Darcian fluid about a vertical full cone embedded in porous media. Journal of Porous Media 2011; 14: 545-553. http://dx.doi.org/10.1615/JPorMedia.v14.i6.80

[19] Bararnia H, Ghasemi E, Domairry G, Soleimani S. Behavior of micro-polar flow due to linear stretching of porous sheet with injection and suction. Advances in Engineering software 2010; 41: 893-897. http://dx.doi.org/10.1016/j.advengsoft.2009.12.007

[20] Bararnia H, Ghasemi E, Soleimani S, Ghotbi AR, Ganji DD. Solution of the Falkner-Skan wedge flow by HPM-Pade'method. Advances in Engineering Software 2012; 43: 44-52. http://dx.doi.org/10.1016/j.advengsoft.2011.08.005

[21] Moghimi SM, Domairry G, Bararni H, Ghasemi E, Soleimani S. Application of homotopy analysis method to solve MHD Jeffery-Hamel flows in non-parallel walls. Advances in Engineering Software 2011; 42: 108-113. http://dx.doi.org/10.1016/j.advengsoft.2010.12.007

[22] Ganji DD, Bararnia H, Soleimani S, Ghasemi E. Analytical solution of the magneto-hydrodynamic flow over a nonlinear stretching sheet. Modern Phy. Letter B 2009; 23: 2541-2556. http://dx.doi.org/10.1142/S0217984909020692

[23] Jalaal M, Ghasemi E, Ganji DD, Bararnia H, Soleimani S, Nejad GM, Esmaeilpour M, Effect of temperature-dependency of surface emissivity on heat transfer using the parameterized perturbation method. Thermal Science 2011; 15: 123-125. http://dx.doi.org/10.2298/TSCI11S1123J

[24] Ghasemi E , Soleimani S, Bayat M. Control Volume Based Finite Element Method Study of Nano-fluid Natural Convection Heat Transfer in an Enclosure Between a Circular and a Sinusoidal Cylinder. Int. J. Nonlinear. Scienc. Numeric. Simulation 2013; 13(7-8): 521-532.

[25] Ghasemi E, Soleimani S, Bararnia H. Natural convection between a circular enclosure and an elliptic cylinder using

Control Volume based Finite Element Method. Int. Commun. Heat. Mass. Trans 2012; 39: 1035-1044. http://dx.doi.org/10.1016/j.icheatmasstransfer.2012.06.016

[26] Kutanaei SS, Ghasemi E, Bayat M. Mesh-free modeling of two-dimensional heat conduction between eccentric circular cylinders. Int.l J. Phys. Scienc 2011; 6(16): 4044-4052.

[27] Seyyedi SM, Soleimani S, Ghasemi E, Ganji DD, gorji M, Bararnia H. Numerical Investigation of Laminar Mixed Convection in a Cubic Cavity by MRT-LBM: Effects of the Sliding Direction. Numerical Heat Transfer A 2013; 63: 285-304. http://dx.doi.org/10.1080/10407782.2013.730456

[28] Soleimani S, Ganji DD, Gorji M, Bararnia H, Ghasemi E, Optimal location of a pair heat source-sink in an enclosed square cavity with natural convection through PSO algorithm. Int. Commun. Heat. Mass. Trans 2011; 38: 652-658. http://dx.doi.org/10.1016/j.icheatmasstransfer.2011.03.004

[29] Moghimi SM, Domairry G, Bararni H, Soleimani S, Ghasemi E. Numerical Study of Natural Convection in an Inclined L-shaped Porous Enclosure. Adv Theor Appl Mech 2012; 5: 237-245.

[30] Bararnia H, Jalaal M, Ghasemi E, Soleimani S, Ganji DD, Mohammadi F. Numerical simulation of joule heating phenomenon using meshless RBF-DQ method. International Journal of Thermal Sciences 2010; 49: 2117-2127. http://dx.doi.org/10.1016/j.ijthermalsci.2010.06.008

[31] Soleimani S, Ganji DD, Ghasemi E, Jalaal M, Bararnia H. Meshless local RBF-DG for 2-D heat conduction: A comparative study. Thermal Science 2011; 15: 117-121. http://dx.doi.org/10.2298/TSCI11S1117S

[32] Jalaal M, Soleimani S, Domairry G, Ghasemi E, Bararnia H, Mohammadi F, Barari A. Numerical simulation of voltage electric field in complex geometries for different electrode arrangements using meshless local MQ-DQ method. Journal of Electrostatics 2011; 69: 168-175. http://dx.doi.org/10.1016/j.elstat.2011.03.005

[33] Soleimani S, Jalaal M, Bararnia H, Ghasemi E, Ganji DD, Mohammadi F. Local RBF-DQ method for two-dimensional transient heat conduction problems. Int Commun Heat Mass. Trans 2010; 37: 1411-1418. http://dx.doi.org/10.1016/j.icheatmasstransfer.2010.06.033

Received on 30-10-2014 Accepted on 10-11-2014 Published on 09-01-2015

DOI: http://dx.doi.org/10.15377/2409-5826.2014.01.02.6